Proceedings of the Fortieth Turbomachinery Symposium
September 12-15, 2011, Houston, Texas

MODELING AND PREDICTION OF SIDESTREAM INLET PRESSURE FOR MULTISTAGE CENTRIFUGAL COMPRESSORS

Jay Koch
Principal Engineer
Dresser-Rand
Olean, NY, USA

Moulay Belhassan
Principal Engineer
Dresser-Rand
Olean, NY, USA

.

Jim Sorokes
Principal Engineer
Dresser-Rand
Olean, NY, USA

ABSTRACT

It is common for some compressors in certain applications to have one or more incoming sidestreams that introduce flow other than at the main inlet to mix with the core flow. In most cases, the pressure levels at these sidestreams must be accurately predicted to meet contractual performance guarantees. The focus of this paper is the prediction of sidestream flange pressure when the return channel outlet conditions are provided. A model to predict the impact of local curvature in the mixing section is presented and compared with both Computational Fluid Dynamics work and measured test data.

INTRODUCTION

Despite recent advances in analytical tools, developers and users of state-of-the-art centrifugal compressor equipment continue to rely heavily on testing to ultimately confirm the performance of new components or stages. This is especially true in heavy hydrocarbon applications such as compressors used in liquefied natural gas (LNG), ethylene, or gas-to-liquid facilities. Heavy hydrocarbon gases have very low gas sonic velocities that produce high Mach numbers in the aerodynamic flowpath. By their nature, such high Mach number, high flow coefficient stages have very narrow flow maps characterized by limited choke and surge margin. In addition, many of these applications require the machines with sidestreams (or sideloads) to accommodate the flows entering and/or exiting the compressor as determined by the particular process for which they are intended. The sidestreams and associated mixing further complicate the performance prediction process because the pressure, temperature and flow conditions at each one of these sidestreams as well as at the exit of the machine must be met within stringent tolerances to optimize the amount of end product delivered by the process. Therefore, it is imperative that the compressor OEM and end user have a firm grasp of the performance characteristics of any impellers, diffusers, return channels, and/or other flow path components used in such equipment.

The high cost associated with delays in the project schedule increase the attractiveness of design and testing methods that ensure these machines meet the contractual operating requirements the first time; without the need for repeated modifications and test iterations to correct performance shortfalls. Given the size, construction style, and in-house test piping arrangements for many large centrifugals, one modification / re-test iteration could take several weeks. Repeated iterations on the OEM's test facility could delay the start-up of a new plant by months, leading to lost production / revenue for the end user as well as lost revenue and reputation for the compressor OEM. Consequently, OEMs spend continually work to enhance their performance prediction methods. This paper details work done toward that end.
This paper is the latest in a continuing series of publications describing work completed in association with a novel test vehicle that was designed to replicate the performance of a full-scale, large frame-size, multi-stage centrifugal compressor for high flow coefficient, high Mach number stages. The test vehicle, described by Sorokes et al (2009), is equipped with a vast array of internal instrumentation that make it possible to evaluate the aero/thermodynamic and mechanical behavior of a compressor. Sufficient instrumentation is installed to allow assessment of the entire compressor as well as individual components or combinations of components. Of particular interest to this study, the test rig included instrumentation at critical locations within the sidestream components to permit an assessment of the losses through each sidestream element.

BACKGROUND

As part of the compressor selection and design process, the OEM must be able to predict the performance of the overall

unit from inlet to discharge flange. For a simple, so-called "straight through" compressor, this means predicting the performance for each stage (inlet guide / impeller / diffuser / return channel or volute) in series from the inlet to the discharge of the machine. However, for units with one or more incoming sidestreams, there is the additional task of accounting for the impact of the sidestream and thereby predicting the conditions at the intermediate flange; i.e., static and total pressure.

Typically, OEMs supply compressor performance curves that reflect flange-to-flange performance because that is what the process engineer needs to ensure proper operation of their system. Such data is easier to monitor when a compressor is installed in the field. However, flange-to-flange data, if not interpreted properly can lead to misleading conclusions as to the relative performance of individual sections of a compression system. For example, if the sidestream losses from the flange to mixing section are attributed to the upstream section, it will cause the upstream section to appear low in performance while the downstream section will show erroneously high performance levels; i.e., efficiency significantly higher than 90%). The need for a more refined method for allocating sidestream losses as well as the need to eliminate other uncertainties regarding the sidestream loss mechanisms has led to additional research on sidestream performance modeling.

Compressor OEM's have completed significant work in recent years to improve their understanding of the flow in sidestreams and sidestream mixing section as well as the impact of the mixed stream on the downstream impeller. In most cases, the portion of the sidestream from the flange connection to the "mixing section" (i.e., the location where the incoming sidestream flow mixes with the core flow) is very similar to a radial compressor inlet. There has been significant work reported in the literature on radial inlets. For example, Flathers et al (1994) compared several geometric variations using Computational Fluid Dynamics (CFD) and measured test results. Koch et al (1995), Kim and Koch (2004), Michelass and Giachi (1997) subsequently reported similar work on different geometric variations. These studies all led to increased understanding of the flow structure and improved prediction methods for inlet losses and the details of the flow field exiting these components. Proper use of the CFD tools also led to more efficient / effective inlet configurations that provided a more circumferentially uniform flow to the downstream impeller. The studies also aided in the one-dimensional prediction of pressure losses.

Additional studies, which included the upstream return channel and the complete sidestream geometry, have been completed to accurately model the flow where the core flow and sidestream flow merge. While this location is typically called the mixing section as noted above, the flows do not completely mix before entering the impeller. The works of Sorokes et al (2000 and 2006) and the prior referenced work on radial inlets have led to a greater comprehension of the complex flows at the sidestream mixing location. However, these works did not address the flow physics that determine the static pressure in the mixing section, which, in turn, sets the flange pressure level. The study by Hardin (2002) describes a one-dimensional method that determines how the flow at the mixing location and, therefore, the local static pressure is impacted by the local flow curvature.

This paper presents predictions for two geometric configurations that violate the assumptions made in previous studies, resulting in a need to modify the relevant equations. Additionally, the prior work did not present the methods used to predict the total pressure downstream of the mixing section. This paper will present various methods to predict the downstream total pressure and compare the analytical results to measured test data on the two geometries.

INVESTIGATIVE STUDY

As part of a recent OEM development program, a study on several sidestream configurations was conducted. The project required compact sidestream mixing sections; i.e., mixing sections that take less axial length; in a compressor with high flow coefficient ($\phi > 0.10$) and high machine Mach number (i.e., U2/A0 > 1.1). The sidestreams were of different sizes as the incoming flows represented different percentages of the flow from the upstream section. The gas density in the sidestreams also varied due to the increasing pressure in the machine. Finally, the machine was tested using a high mole weight refrigerant to replicate the high gas densities and Mach numbers. Representative geometry for a typical configuration is shown in Figures 1a and 1b.

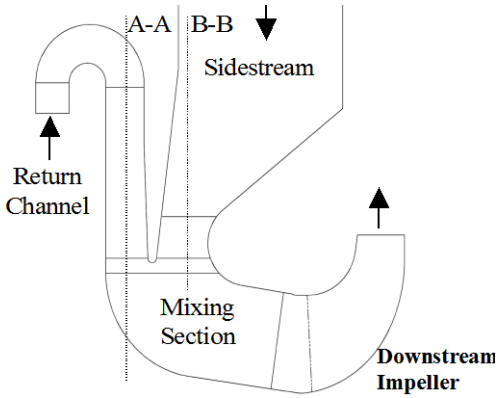

Figure1a. Geometry for configuration 1

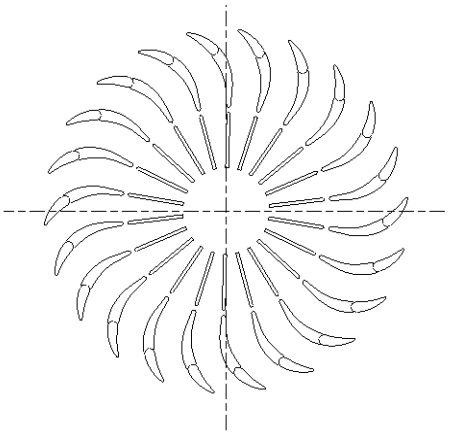

Figure1b. Geometry for configuration 1 – section A- A

During the detailed design process, each proposed stage geometry was modeled using a commercially available CFD code, ANSYS CFX-10. As part of this study, the sidestream inlet geometry was optimized within the available axial space provided. The CFD domain for each sidestream included the upstream diffuser, return channel, sidestream nozzle, sidestream plenum, mixing section, and downstream impeller. The full 360-degree model included all passages to evaluate any circumferential flow non-uniformity at the exit of the sidestream. The upstream impeller was not included to reduce the size of the computational domain, thereby reducing solution time. This simplification also allowed the return channel exit conditions to be varied for different flow conditions; i.e., to replicate the flow conditions from maximum (choke) to minimum stable flow (stall / surge). Because the objective of the study was to predict the sidestream flange pressure, when provided return channel exit conditions, it was felt this simplification would have a minimal impact on the flow physics of interest.

The geometry was modeled using a combination of hexahedral and tetrahedral elements. All axisymmetric components, such as the diffuser and return channel, were modeled using hexahedral elements and the non-uniform components, such as the sidestream nozzle and plenum section, were modeled using tetrahedral elements because such components are more easily modeled using “tets”. The grids were refined for each component and grid element type as it is recognized that higher grid densities are required for tetrahedral as opposed to hexahedral elements. Each component had a grid size of approximately 2 million elements and the total grid size was approximately 6 million elements. For the sidestream inlet, the grid density used is similar to those reported by the current authors in Kim and Koch (2004).

The boundary conditions of the model were based on the one-dimensional predictions used to select and size the hardware. The prescribed flow angle, total pressure and total temperature were specified at the diffuser entrance. Total temperature and mass flow were specified at the sidestream entrance and total mass flow was specified at the exit of the computational domain. The inlet pressure at the sidestream entrance was the objective function of the analysis.

A second order discretization scheme was used for the simulation and standard k-ε model was adopted as a turbulence model combined with a scalable wall function approach that eliminates the necessity of discretely resolving the large gradients in the thin, near-wall region. The convergence criterion was set to the maximum residual of 10^{-4} for u, v, w, and p.

For the two sidestream configurations addressed in this paper, the internal elements, return channel vanes, sidestream vanes and inlet guide vanes, were fixed during the optimization. Only the meridional passage width was varied.

In the first configuration (designated Configuration 1), the core flow (i.e., flow exiting the upstream return channel) and incoming sidestreams flows were nearly equal. This geometry is shown in Figures 1a and 1b. The second configuration (Configuration 2) was for a higher pressure and hence higher density stage and had a core flow that was much greater than the sidestream flow. The details of this mixing section geometry can be seen in Figure 2.

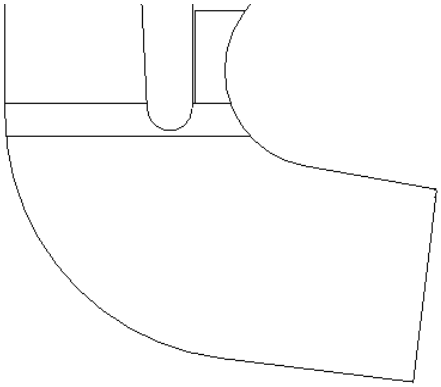

Figure 2. Mixing section geometry for configuration 2

The design values of area ratio (return channel exit area to sidestream exit area), density, and return channel exit Mach number are provided in Table 1.

Table 1. Sidestream Design Parameters

Configuration	Density lb/ft^3	Area Ratio Main/Sidestream	Mach Number
1	0.30	0.76	0.34
2	1.00	4.96	0.26

The results of the CFD study are shown in Figures 3-6. The Mach number distribution in the sidestream nozzle for configuration 1 is shown in Figure 3. This configuration shows the vane rows in the sidestream are oriented with the flow to provide a circumferentially uniform velocity profile at the exit of the sidestream. A meridional view providing the Mach number distribution in the mixing section is shown in Figure 4. This plot shows a variation in the Mach number across the sidestream exit. The variation in Mach number is also evident at the exit of the return channel as the flow turns to enter the downstream impeller.

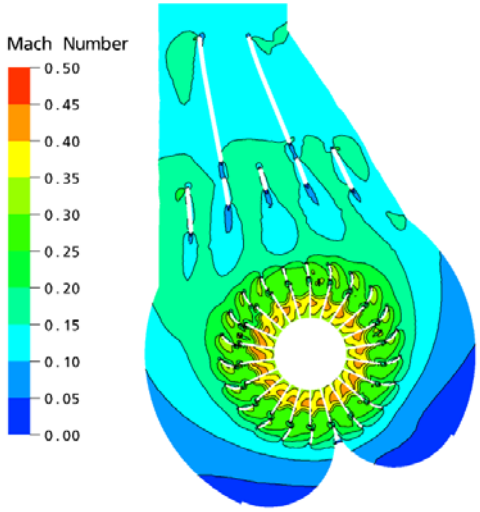

Figure 3. Mach number in sidestream – configuration 1

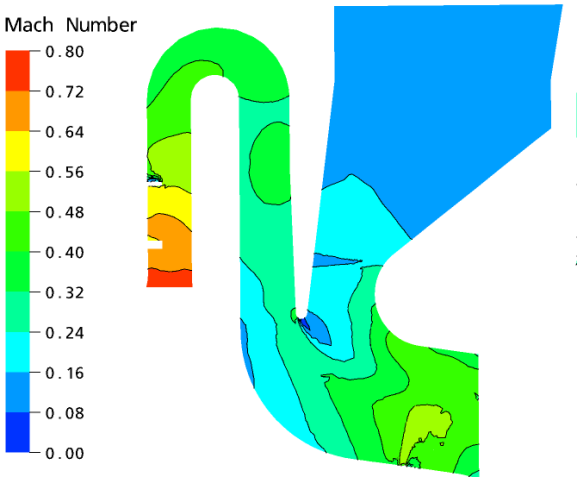

Figure 4. Mach number at sidestream mixing location - configuration 1

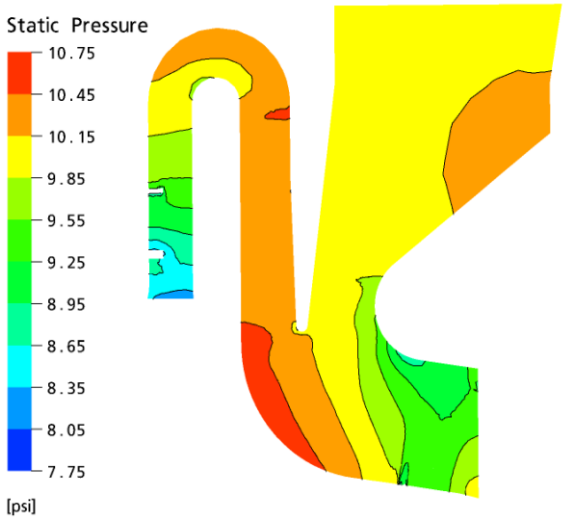

Figure 5. Static pressure at the sidestream mixing location - configuration 1

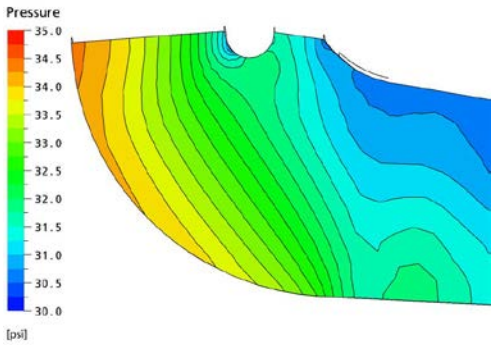

Figure 6. Static pressure at the sidestream mixing location – configuration 2

Contours of the static pressure at the same location are shown in Figure 5. It is evident from this figure that the static pressure varies from the shroud wall at the exit of the sidestream to the hub wall downstream of the return channel. Because of the lower static pressure at the sidestream exit, the total pressure at this location is lower even though the velocity upstream of the curvature is roughly matched for both streams.

This phenomenon of reduced pressure at the sidestream exit was predicted by Hardin (2002). Based on the relationships shown in that work, this variation in pressure can be expected to increase with dynamic pressure, $\rho V^2/2$, and with larger variations in curvature between the two streams.

A plot of static pressure for configuration 2 is shown in Figure 6. This configuration shows similar trends to configuration 1 with significant variation in the static pressure from the exit of the return channel to the exit of the sidestream.

In reviewing these configurations it is evident that the specific formulation developed in the prior work does not apply to this geometry. A major assumption put forth in the prior work was that there was no variation in the static pressure at the outlet of the return channel passage. Thus the effect of curvature was only applied across the sidestream exit. For this geometry, the formulation must be modified to account for the variation across both the return channel exit and the sidestream exit. While simple in nature, this can have a significant impact on the predicted static pressure at the sidestream exit.

Before developing a method to account for the changes in curvature, an optimization study was conducted on the mixing section of configuration 2. To reduce the execution time and allow for more design iterations, a sub-model was created that included a portion of the return channel vane exit and a portion of the exit of the plenum section of the sidestream just upstream of the mixing section. The upstream diffuser and return channel as well as the sidestream plenum were removed from the sub-model. This also allowed the geometry to be modeled as a pie slice section as opposed to a full 360º model. Comparison of sub-model and full model solutions revealed that the simplified model captured the important flow features in the mixing section. Therefore, the simplified model was used for the optimization study for the mixing section.

PREDICTION METHODOLOGY

To accurately predict the sidestream exit conditions, proper boundary conditions for the problem must be established. The exit conditions at the return channel are generally known from one-dimensional predictions or from test measurements. Therefore, for this discussion it was assumed the discharge total pressure was known at the exit of the return channel preceding the mixing section. Additionally, it is assumed the area, flow rate, temperature and gas properties were known at the return channel exit and at the sidestream exit.

Given the referenced information, the return channel exit mean velocity and static pressure can be calculated. Based on basic flow principles, it was assumed that the static pressure was equal between both flow streams at the mixing location. The only location where this is true is at the shroud wall at the exit of the return channel and the hub wall at the exit of the sidestream. This assumption is supported by the previous computational study completed by the OEM and by other

researchers such as Hardin (2002). Unfortunately, the pressure at this location is not as desired because of the local curvatures in the mixing section. The desired result can be obtained via a series of equations that allow the average static pressure at the exit of the sidestream to be calculated from the average static pressure at the exit of the return channel.

According to basic aerodynamic principles, the relationship of pressure versus radius of curvature can be expressed by Equation (1).

$$\frac{dP}{dR} = \frac{\rho V^2}{R} \qquad (1)$$

For the geometry shown in Figure 7, the average static pressure at the exit of the return channel can be related to the average pressure at the exit of the sidestream by the variation in curvature using Equation 1. The average static pressure at the sidestream exit is defined by Equation (2).

$$P_{s_{ss}} = P_{s_{Ret}} + \frac{\rho V^2 \left(R_{c_{Ret}} - R_{c_{ss}}\right)}{R_{c_{Ret}}} \qquad (2)$$

Where:

$P_{s_{ss}}$ = Static pressure at sidestream exit
$P_{s_{Ret}}$ = Static pressure at return channel exit
$R_{C_{ss}}$ = Radius sidestream of curvature (see fig. 7)
$R_{C_{Ret}}$ = Radius of return channel curvature (see fig. 7)
ρ = Gas density
V = Velocity at the sidestream exit

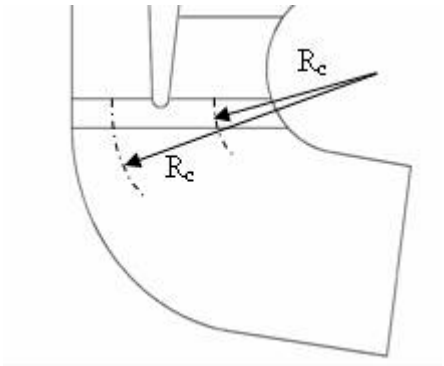

Figure 7. Geometry for pressure prediction

Once the static pressure at the sidestream exit is determined, the velocity and total pressure can be calculated. The flange total pressure can be calculated based on the predicted losses in the nozzle plenum region, once the sidestream exit total pressure is known (Equations (3) and (4)). The losses in this region of the sidestream have been shown to be consistent and predictable by 1-D models. The 1-D model for a given geometry can be based on CFD prediction or based on test measurements.

$$P_{T_{ss}} = P_{s_{ss}} + \frac{\rho V^2}{2} \qquad (3)$$

$$P_{T_{FLG}} = P_{T_{ss}} + \frac{\rho V_{FLG}^2}{2} LC_{ss} \qquad (4)$$

Where:

$P_{s_{ss}}$ = Static pressure at sidestream exit
$P_{T_{ss}}$ = Total pressure at sidestream exit
$P_{T_{FLG}}$ = Total pressure at flange
ρ = Gas density
V = Velocity at sidestream exit
V_{FLG} = Velocity at flange
LC_{ss} = Loss coefficient

The appropriate method for the prediction of the total pressure downstream of the mixing section at the inlet of the impeller has not been questioned in the literature. The appendix of the test standard from ASME (1997), defines a momentum balance method, but this method is approximate. Attempts to use this method have not been very successful for these authors or others in the open literature. The impact of the gradient in total pressure on the downstream impeller performance varies greatly. Some CFD studies indicate a significant impact on performance while other studies show a minor impact. For 1-D performance prediction purposes a single representative value of the impeller inlet pressure is desired. This representative pressure should provide a consistent reference between predicted performance and measured test results. It is also desired that the selected value provides a consistent reference for comparison between performance prediction and measured test results.

When CFD results are evaluated, a mass-averaged total pressure at a selected plane is the common method for evaluation. Evaluations of test results often use an arithmetic average or area average based on total pressure measured by a single pressure probe or multi-hole pressure rake. The prior work by Hardin (2002) suggests mass-averaging the total pressure at the exit of each stream. To determine which method provides a more consistent result, a set of evaluation criteria was developed for use on future development tests. The test results will be evaluated using the three methods listed above to determine which method provides a more consistent result and therefore used for future comparisons between test results and analytical predictions.

TEST DATA AND DISCUSSION

After completion of the design study, the OEM constructed a full-scale development test rig; again, see Sorokes et al (2009). As noted, the flow path of the test rig was heavily instrumented to allow the measurement of the aero-thermodynamic performance of the components of each stage including the sidestream elements. The internal instrumentation included total pressure probes, dynamic

pressure probes, total temperature probes, and five-hole probes, which measure both pressure and flow direction. A schematic of the internal instrumentation layout used for each compressor stage is given in Figure 8.

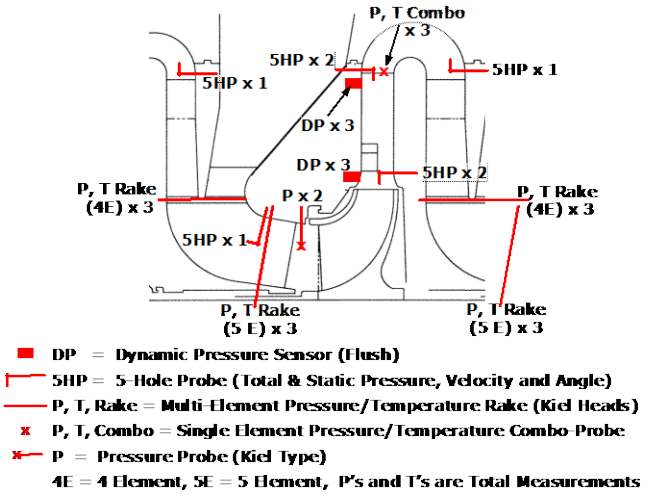

Figure 8. Test rig internal instrumentation layout

For each sidestream, the total pressure and temperature were measured at the exit of the return channel and at the sidestream exit. Additionally, the total pressure and temperature distributions were measured near the exit of the mixing section; i.e. just upstream of the impeller; via pressure and temperature rakes. Therefore, it was possible to assess the hub-to-shroud variation (or stratification) in pressure and temperature due to the core / sidestream flow mixing.

In addition to the internal instrumentation, the total pressure, total temperature and mass flow were measured at the flange locations using standard combination pressure / temperature probes.

All performance testing was conducted using R-134A refrigerant to achieve aerodynamic similitude at the design conditions. The test measurements for each sidestream were taken in accordance with the ASME PTC-10 test code from ASME (1997).

To evaluate the revised prediction scheme, the predicted sidestream exit total pressure was calculated at the test conditions and compared with the measured total pressure on test. The prediction was based purely on the known geometry and test conditions.

For each sidestream configuration, data is presented for different flow rates at a fixed impeller tip Mach number of 1.10. The flow ratio between the sidestream and the core flow is maintained for all operating points using the OEM stringent guidelines; i.e., more restrictive than the standard ASME Power Test Code (see Kolata and Colby (1990)). The temperatures for core flow and incoming sidestream streams were kept equal to avoid heat transfer that would add uncertainty to the efficiency calculation.

The results of the prediction for configuration 1 are shown in Figure 9.

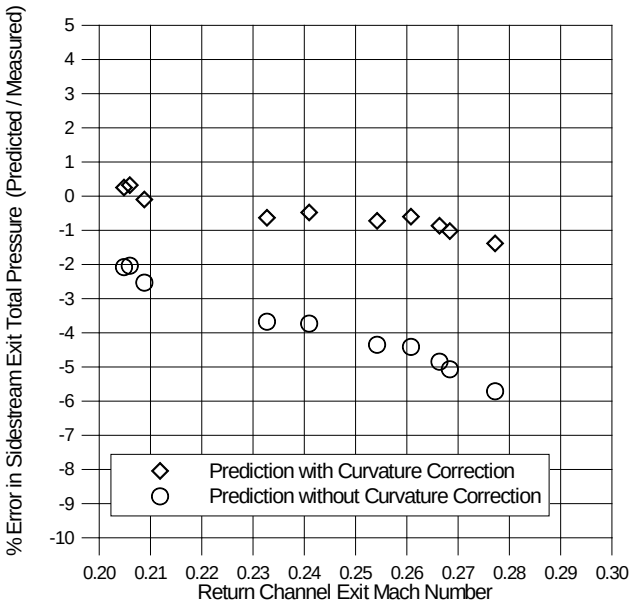

Figure 9. Error between test and measurement with and without curvature correction – configuration 1

The percent error in the sidestream exit predicted total pressure versus Mach number at the outlet of the return channel is shown. For configuration 1 the prediction model is within ±1.5% of the test results. As a means of determining the suitability of this calculation, the percent error in sidestream total pressure was also calculated without the curvature correction. This comparison showed the sidestream exit total pressure was always over-predicted without the curvature correction. For this application, failure to account for the curvature effects resulted in an error of up to 5.8%. Similar results for configuration 2 are shown in Figure 10.

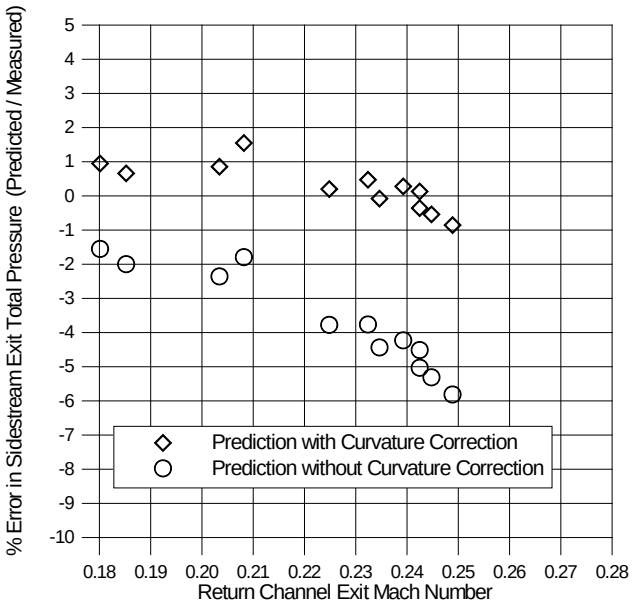

Figure 10. Error between test and measurement with and without curvature correction – configuration 2

For configuration 2, the prediction model accounting for curvature is also within ±1.5% of the test results. The error without the curvature correction is even greater than on configuration 1, with a maximum difference of more than 6.1%.

Because there was considerable interest in the performance of the sidestream and downstream impeller with off-design flow functions, a set of conditions was defined to investigate such operating conditions. These additional data provided insight into prediction of the impeller inlet total pressure downstream of a sidestream for off-design conditions.

During these tests the unit was intentionally tested at core flow to sidestream flow ratios that were at the limits of the ASME test standard (i.e., ±10%), and thus considerably different than the design values. Based on the curvature prediction model, the flow function variation causes the sidestream exit pressure (and thus flange pressure) to vary from the design conditions. This would be true even if the downstream impeller inlet conditions remain unchanged.

The change in flange pressure due to the different flow ratios leads to variations in the calculated section performance even though the impeller / diffuser / return channel performance remains essentially unchanged. Recall that it was possible to determine the performance from impeller exit to return channel exit because of the additional instrumentation available in the test vehicle. The internal performance (based on impeller inlet to return channel exit) and the flange to flange performance are shown in Figure 11 for the same operating conditions. There are small changes in the internal performance for the various sidestream flow ratios, most likely due to the impact on varying impeller inlet velocity profile due to "mixing effects" at the off-design flow ratios. However, there are more noticeable differences in the flange to flange calculation, particularly toward the high capacity end of the map.

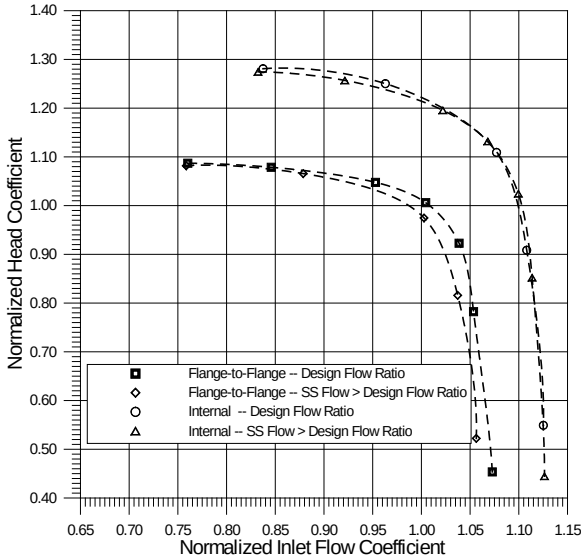

Figure 11. Flange to Flange and Internal Head Coefficient for various sidestream flow ratios

As part of the prediction method discussion, data from these tests were also used to evaluate which method of determining the downstream impeller inlet condition provides the best correlation with the test results. To complete this comparison, the impeller inlet condition was calculated three ways. The first method was based on a mass-average of the total pressures at the outlet of the return channel and the sidestream exit. The second method used an arithmetic average of the total pressure rake downstream of the mixing section. The third method was based on an area average of the downstream rake pressures.

All three methods were compared using polytropic head coefficient, μ_p, versus inlet flow coefficient, ϕ, (see Figure 12).

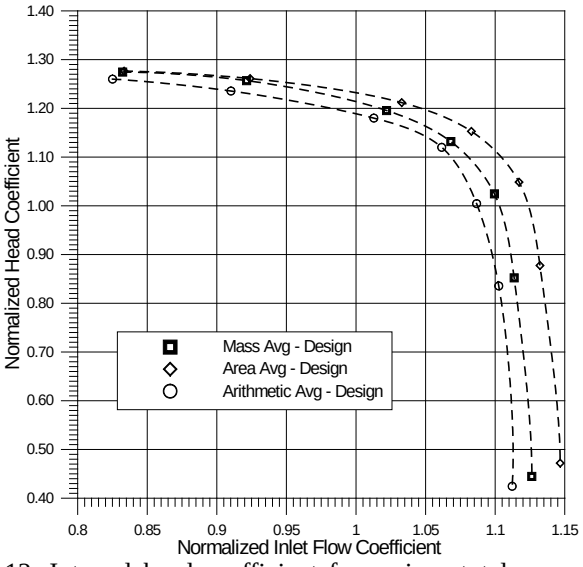

Figure 12. Internal head coefficient for various total pressure averaging methods at the mixing section

The data was normalized using the design point head and flow coefficient and trends were reviewed for both design flow and off-design flow conditions (i.e., from overload to stall/surge). For each case, the basic impeller inlet similarity condition remained the same. That is, the compressor was run at the same tip Mach number, and Reynolds number. However, the sidestream flow function was allowed to vary within the limits of the ASME test code. As can be seen in the curves, the different averaging methods did result in a change in the perceived performance. This is not overly surprising because the different averaging methods will result in a different inlet pressure to the downstream impeller and because the head coefficient is directly dependent on the inlet pressure, the resulting variation in head coefficient is to be expected.

Specifically, the change in inlet pressure due to the various averaging techniques caused a shift in the inlet capacity and also caused a change in the head coefficient as well as a change in rise-to-surge for the area average method. The area-averaged method predicts a larger capacity and pressure coefficient than either method. The mass-averaged result falls between the two other methods. Based on this comparison, each method would appear to provide a consistent basis for comparison with predictions. The mass-averaged method has the advantage of using a measured quantity that has less variation hub to shroud than the other methods and is less sensitive to the flow ratio of the core flow to the sidestream flow. Finally, the mass-averaging method also allows for a direct comparison between

one-dimensional predictions, CFD and test results, as the required information is typically readily available.

CONCLUSIONS

This paper presents results from a recent sidestream design study and compares the analytical results to test measurements. The new method builds on the prior works of Hardin (2002), Sorokes et al (2000) and Sorokes et al (2006). Based on this study, a modification to the published methodology has been proposed to improve the calculation of the inlet pressure for standard incoming sidestreams. Using the new method, it is possible to predict the sidestream exit pressure within an accuracy of ±1.5%. This method enhancement will make it possible to provide more accurate sidestream pressure levels, thereby improving the process modeling for new or upgraded facilities.

The comparison of test results with different averaging methods has shown that each method offers consistent, though somewhat different result. Based on this study, it is felt that mass averaging of the core flow pressure and the sidestream pressure provides the most effective reference for correlation of the impeller inlet total pressure.

DISCLAIMER

The information contained in this document consists of factual data, and technical interpretations and opinions which, while believed to be accurate, are offered solely for informational purposes. No representation or warranty is made concerning the accuracy of such data, interpretations and opinions.

NOMENCLATURE

V = Velocity
R = Radius of Curvature
N = Rotational Speed
D = Impeller Outer Diameter
Q = Volume Flow
U = Tip Speed, π DN
n = Polytropic Exponent, $\frac{\ln\left(\frac{P_2}{P_1}\right)}{\ln\left(\frac{\upsilon_1}{\upsilon_2}\right)}$
ρ = Density
υ = Specific Volume
ϕ = Inlet Flow Coefficient, $\frac{Q}{2\pi ND^3}$
μ = Polytropic Head Coefficient, $\frac{\frac{n}{n-1}\left(P_2\upsilon_2 - P_1\upsilon_1\right)}{U^2}$
P_T = Total Pressure
P_S = Static Pressure
T_T = Total Temperature
Ret = Return Channel Exit
SS = Sidestream Exit
Flg = Sidestream Flange

REFERENCES

ASME, PTC 10, 1997, Performance Test Code on Compressors and Exhausters, @ ASME Press.

Flathers, M., Bache, G., Rainsberger, R., 1994, An Experimental and Computational Investigation of Flow in a Radial Inlet of an Industrial Pipeline Centrifugal Compressor, @ ASME 94-GT-134.

Gilarranz, J., 2007, Actuation and Control of a Movable Geometry System for a Large Frame-Size, Multi-Stage Centrifugal Compressor Test Rig, @ ASME Paper GT2007-27592, Submitted for Presentation at the GT2007, ASME Turbo Expo 2007, Montreal, Canada.

Hardin, James R., 2002, A New Approach to Predicting Centrifugal Compressor Sideload Pressure, @ IMECE2002-39592, Proceedings of ASME International Mechanical Engineering Congress & Expo, 2002, New Orleans, USA.

Kim, Y., Koch, J., 2004, Design and Numerical Investigation of Advanced Radial Inlet for a Centrifugal Compressor Stage, @ IEMCE2004-60538, Proceedings of ASME International Mechanical Engineering Congress & Expo, 2004, Anaheim, CA, USA.

Koch, J., Chow, P., Hutchinson, B., Elias, S., 1995, Experimental and Computational Study of a Radial Compressor Inlet, @ ASME 95-GT-82.

Kolata, J. P., and Colby, G. M., 1990, Performance and Sidestream Testing, @ Proceedings of the 1990 Dresser-Rand Technology Seminar, Olean, NY.

Michelass, V., Giachi, M., 1997, Experimental and Numerical Analysis of Compressor Inlet Volutes, @ ASME 97-GT-481.

Sorokes, J., Kopko, J., Koch, J., 2006, Sidestream optimization for LNG compressor applications, @ European Fluid Machinery Congress.

Sorokes, J., Nye, D., D'Orsi, N., Broberg, R., 2000, Sidestream Optimization Through the Use of Computational Fluid Dynamics and Model Testing, @ Proceedings of the Twenty-ninth Turbomachinery Symposium, Thurbomachinery Laboratory, Texas A&M University, College Station, Texas, pp. 21-30.

Sorokes, J.M., Soulas, T., Koch, J.M., Gilarranz, J. L., 2009, Full- Scale. Aerodynamic And Rotordynamic Testing For Large Centrifugal Compressors, @ Proceedings of the Thirty Eighth Turbomachinery Symposium, Thurbomachinery Laboratory, Texas A&M University, pp. 71-80.

ACKNOWLEDGEMENTS

The authors thank Dresser-Rand Company for funding this overall project and for allowing the publication of this work.